A Simulation of the Effects of High Strain Energy Storage in Large Plastic Structures

V. L. GROSHANS *and* M. T. TAKEMORI

Polymer Physics and Engineering Branch
Corporate Research and Development
General Electric Company
Schenectady, New York 12301

Brittle failures of large plastic structures observed in the field may have occurred at much higher loads than implied from the fracture surfaces, indeed, as if very ductile failures had occurred. It has been demonstrated that these brittle failures may be a direct result of high energy storage upon impact in large compliant systems. A rubber-toughened blend of polybutylene terephthalate (PBT) and polycarbonate (PC) was highlighted in this study. Soft steel springs were used in series with compact tension samples to simulate the high energy-storing capability of large compliant structures. Ductile and stable fractures of compact tension samples of the blend were observed at all of the temperatures tested down through −30°C. With the insertion of springs to simulate large compliant structures, however, unstable failures resulted. At 25°C, initial ductile crack growth was followed by ductile but unstable failure. At −30°C, initial ductile crack growth was followed by brittle unstable failure. These instabilities resulted from the excessive amount of stored energy released by the system during initial crack growth. A higher rubber variant of the PBT/PC blend as well as acrylonitrile-butadiene-styrene (ABS) and polycarbonate exhibited similar behavior.

INTRODUCTION

Brittle, explosive failures of large plastic structures have been observed under certain conditions. This behavior cannot necessarily be attributed to a truly brittle failure distinguished by fractures at very low loads. It has been demonstrated that these failures may be occurring at much higher loads than implied from the fracture surfaces, indeed, as if very ductile failures had occurred.

Large, compliant structures store large amounts of strain energy on application of external forces. This behavior serves to absorb the impact of the forces. If flaws are present at the time of impact, however, the stored energy can drive these flaws in explosive proportions. The brittle, explosive failures observed may be a direct result of this stored energy.

A rubber-toughened blend of polybutylene terephthalate and polycarbonate (PBT/PC) was highlighted in this study. Soft steel springs were used in series with compact tension samples to simulate the high strain energy-storing capability of large plastic structures. To understand the general behavior of rubber-toughened polymer blends, different temperatures, rates, and rubber contents were studied.

Acrylonitrile-butadiene-styrene (ABS) and polycarbonate were also tested to demonstrate the behavior common to all large compliant structures.

BACKGROUND

The stress intensity factor, K, is proportional to the magnitude of the stress field around the crack tip in a linear elastic body. The equation relating specimen geometry, crack length, and load to the stress intensity factor for a compact tension sample is as follows (1):

$$K = (P/BW^{1/2})[(2 + a/W)(.886 + 4.64a/W - 13.22a^2/W^2 + 14.72a^3/W^3 - 5.6a^4/W^4)/(1 - a/W)^{3/2}] \quad (1)$$

where P = load, B = sample thickness, W = sample width from load line, and a = initial crack length.

The relationship between the load and the displacement for the fracture of compact tension samples is illustrated in *Fig. 1*. When referring to a truly brittle failure, a linear relationship between load and displacement is implied with a rapid, unstable fracture at a relatively low load (curve A). A completely ductile failure, illustrated by curve B, implies a gradual stable tearing of the material with a much higher maximum load. A third distinguishing behavior is illustrated by curve C. The initial ductility and maximum load are nearly identical to that of curve B; however, beyond the maximum load, the sample experiences a rapid, unstable drop to zero load. This behavior occurs when large amounts of strain energy are stored in the system, such as in a large compliant structure. Upon initial ductile crack growth, the stored energy is released and the crack is driven open at disproportionate speeds. Thus, the sample initially experiences a slow stable tearing, followed by rapid, unstable growth. This unstable growth, dependent on the conditions of testing and the material toughness, can result in ductile or brittle fracture surfaces. These relationships are more clearly illustrated by fracture tests of polycarbonate compact tension samples (see *Appendix A*). A simple graphical interpretation of crack instability is presented in *Appendix B*.

EXPERIMENTAL

All of the tests were performed on an Instron 1350 servohydraulic testing machine and the results were recorded onto a Nicolet Explorer IIIA digital oscilloscope. A crack opening displacement (COD) gauge monitored the displacements at the crack mouths of the compact tension samples. Low temperatures were achieved by a constant influx of liquid nitrogen into an oven that enclosed the experimental apparatus. A temperature controller maintained the desired temperature within 0.5°C.

Samples of a 50/50 blend of PBT/PC with 10% rubber were obtained in the form of 20 by 15 by 0.64-cm injection-molded plaques. Compact tension (CT) samples were machined from the side opposite the plaque molding gate. Each sample was prepared so that the crack was oriented normal to the direction of resin flow inherent in the injection-molding process. The CT samples were machined from these plaques using the ASTM E-399 sample preparation guidelines (see *Fig. 2* and *Ref. 1*). However, a sample thickness of 0.64 cm was used instead of the 1.02-cm sample thickness required by the ASTM guidelines to ensure plane strain fracture conditions. Since our objective was to observe instabilities in ductile crack growth rather than to induce the plane strain brittle failures, this discrepancy was not critical to the testing. In a similar vein, peak load values were used to calculate corresponding K-values (using *Eq 1*) to characterize the fracture tests in this study, since neither K_{IC} nor K_{init} was the object of interest for these tests.

Sharp cracks were used in the compact tension samples to illustrate the most severe conditions. The sharp cracks were prepared by fatigue loading from a razor-notched crack at room temperature. Before fatiguing, a high compressive load was momentarily applied to the notch to help initiate fatigue growth. The sinusoidal loading was then performed at a frequency of 10 Hz with an applied maximum load (determined from *Eq 1*) necessary to produce a maximum K-value of 2.5 MN/m$^{3/2}$ at the crack tip. A minimum fatigue load was chosen such that the ratio of minimum load to maximum load was approximately equal to 0.1. The fatigue cracks were grown approximately 0.5 cm from an initial razor indentation to a final crack length of approximately 0.5W. This procedure ensured that the fatigue cracks were of sufficient length to avoid any adverse effects from the initial machining and notching processes. Blunt cracks of known crack tip radii, which

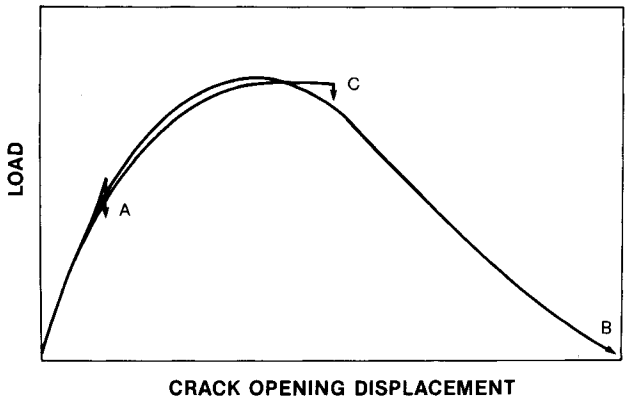

Fig. 1. Model fracture behaviors.

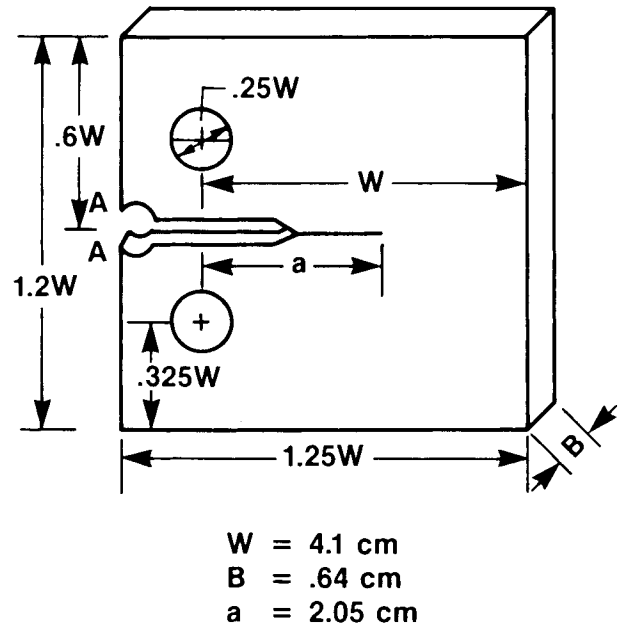

Fig. 2. Compact tension sample.

represent less severe conditions, were prepared in the CT samples by drilling the appropriate size drill bit at the tip of a saw cut to produce a final crack length of $0.5W$.

Large compliant samples (structures) were simulated on a laboratory scale by placing soft steel springs in series with the small test samples. Because of the series loading arrangement, the springs experienced the same load as the small test samples and acted as reservoirs of elastic strain energy. A matched pair of springs was selected with a net compliance of 44 μm/N, which is an order of magnitude higher than that of the CT samples tested. The springs thus stored roughly 10 times more strain energy than the series-loaded CT samples. A simulated large compliant structure (CT sample in series with the springs) is depicted in *Fig. 3.*

After sample preparation, the samples were individually placed in the Instron with the COD gauge situated at the mouth of each sample (*Fig. 2*, location AA). The samples were then fractured in tension at a constant piston displacement rate. Solitary CT samples of the PBT/PC blend as well as the CT samples in series with two soft steel springs were fractured at several different rates and temperatures. Selected fracture tests were also performed on ABS and a higher rubber variant (14%) of the PBT/PC blend.

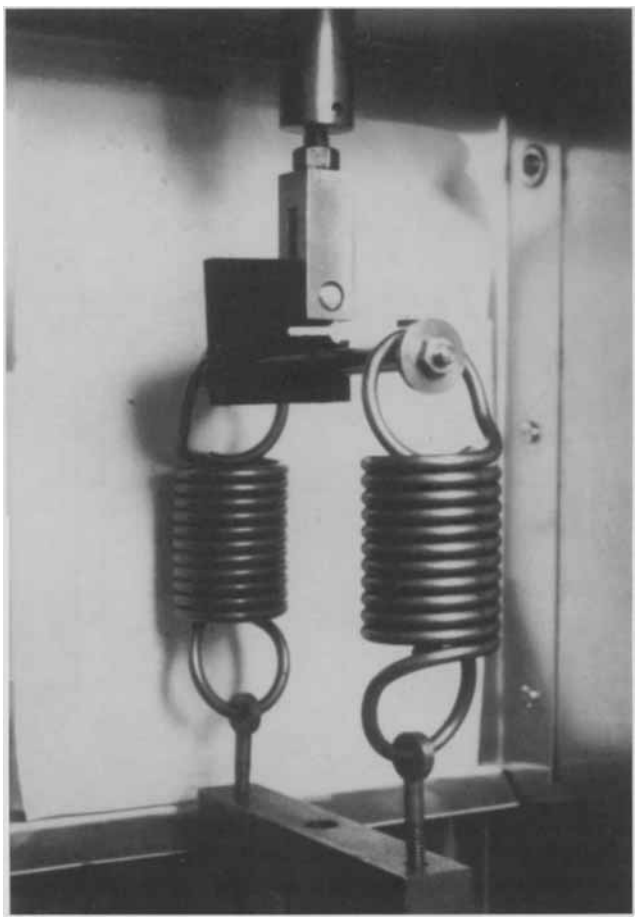

Fig. 3. Experimental apparatus: a compact tension sample in series with springs.

RESULTS

Typical load vs. crack opening displacement data for the 10% rubber-toughened PBT/PC blend are plotted in *Figs. 4–7. Figure 4a* represents the temperature dependence of the fracture of CT samples with fatigue-prepared crack lengths approximately equal to $0.5W$. Testing was conducted on both the solitary CT sample and the CT sample in series with springs (the simulated large part). At room temperature (25°C) and a constant piston displacement rate of 0.254 cm/s, the samples without and with springs experienced similar initial compliances and peak loads with K-values of 6.2 MN/m$^{3/2}$ and 6.4 MN/m$^{3/2}$, respectively (*Fig. 4a*, curves A and B). Both samples possessed similar ductile fracture surface appearances (see *Fig. 4b*). The solitary CT sample exhibited a stable, gradual decrease from maximum to zero load. The simulated large part, however, exhibited a ductile unstable behavior (a rapid drop from a high load to zero load). This unstable behavior is a result of the additional energy that is elastically stored in the springs during loading. When the

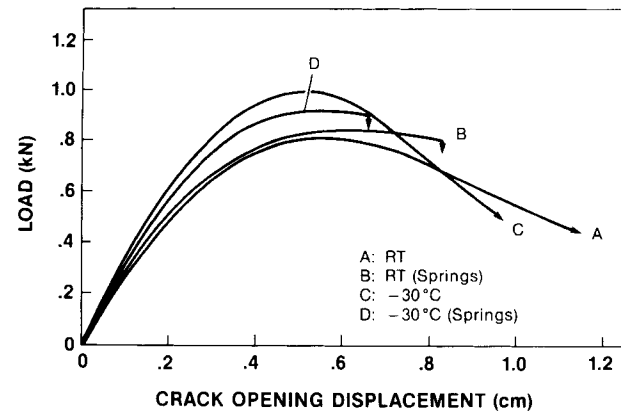

Fig. 4a. Fracture of PBT/PC (10% rubber) at 0.254 cm/s as a function of temperature.

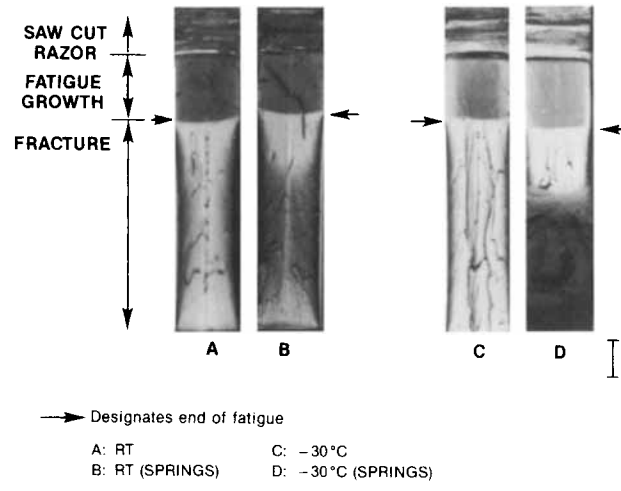

Fig. 4b. Fracture surfaces at 0.254 cm/s.

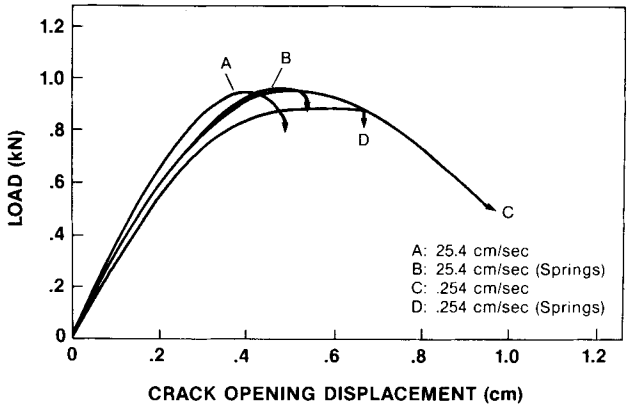

Fig. 5a. Fracture at −30°C as a function of rate.

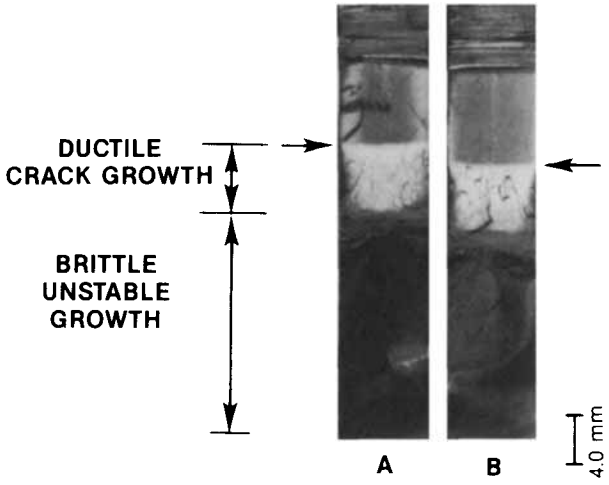

Designates end of fatigue
A: 25.4 cm/sec
B: 25.4 cm/sec (Springs)

Fig. 5b. Fracture surfaces at −30°C and 25.4 cm/s.

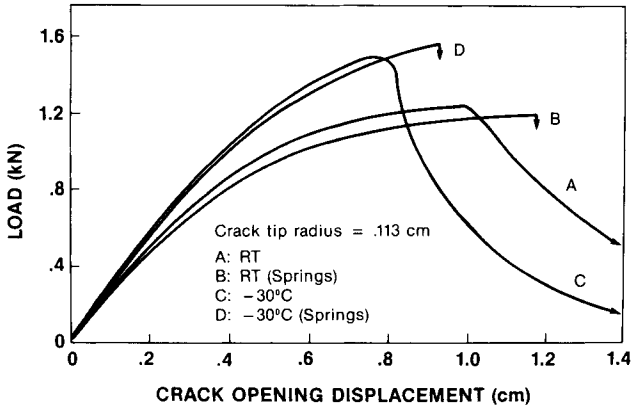

Fig. 6. Fracture with blunt crack tips at 0.254 cm/s as a function of temperature.

critical load for fracture is reached, slow ductile growth begins at the crack tip, which causes a contraction of the springs and a partial release of the stored elastic energy. The crack, in an attempt to absorb the excessive amount of energy released by the system, is driven open at

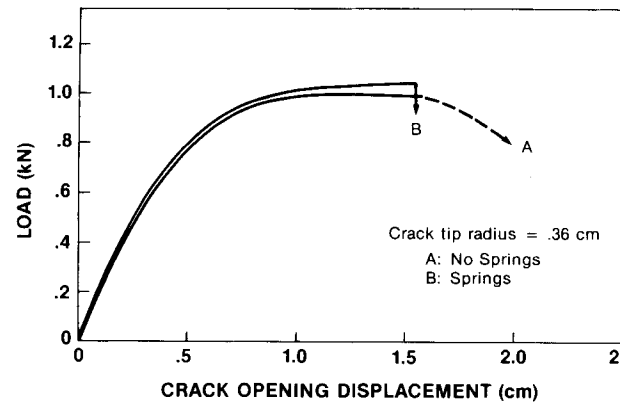

Fig. 7. Fracture with severely blunted crack tips at 25°C and 0.254 cm/s.

disproportionate speeds. The result is unstable fracture.

Fracture tests conducted at −30°C and 0.254 cm/s (*Fig. 4a*, curves C and D) resulted in similar initial compliances and maximum loads with K-values of 7.2 MN/m$^{3/2}$ for the system with no springs and 7.1 MN/m$^{3/2}$ for that with springs. The solitary CT sample again fractured stably, showing little difference from the 25°C sample. The simulated large part, however, experienced a brittle unstable failure after initial ductile crack growth and the sudden release of excessive stored elastic energy. The striking differences between the ductile and brittle surface appearances at −30°C can be seen in *Fig. 4b*.

The rate dependence of the toughened PBT/PC blend at −30°C is demonstrated in *Fig. 5a*. Curves C and D of *Fig. 5a* are the test results at −30°C and 0.254 cm/s reproduced from *Fig. 4a*, curves C and D. Curves A and B of *Fig. 5a* represent data from similar testing performed at −30°C and 25.4 cm/s. At the faster rate, both the CT sample without springs (curve A) and that with springs (curve B) experienced brittle unstable failures after initial ductile crack growth (fracture surfaces presented in *Fig. 5b*). Thus, at the faster rate, neither CT sample was capable of absorbing in a controlled manner the stored energy released by the system.

The effects of crack tip sharpness were examined by testing CT specimens with blunt cracks instead of sharp fatigue cracks. *Figure 6* demonstrates the temperature dependence of samples with blunt cracks (crack tip radius equal to 0.113 cm and total crack length approximately equal to 0.5W) fractured at a piston displacement rate of 0.254 cm/s. Curves A and B are the room temperature test results for the CT specimen without springs and with springs, respectively, and curves C and D are the test results at −30°C. Similar behavior is observed as that shown in *Fig. 4*. As with the fatigued samples, the solitary CT samples with blunt cracks experienced ductile stable fractures. In addition, the simulated large part at room temperature experienced a ductile unstable frac-

ture while that at −30°C fractured in a brittle unstable manner. Because of extensive plastic flow around the blunt crack tips before crack initiation, the maximum loads and the crack opening displacements of the blunt-crack samples were both approximately 30% larger than those of the sharp-crack samples for the respective conditions.

Samples with even blunter cracks (crack tip radius equal to 0.36 cm and crack length approximately equal to 0.55*W*) were similarly tested at room temperature and 0.254 cm/s (see *Fig. 7*). The gradual dissipation from maximum load to zero load for the no-spring system (curve A) and the sudden drop from maximum load to zero load for the spring system (curve B) were again present. Both fracture surfaces possessed the same ductile appearance.

The PBT/PC blend with 14% rubber content was similarly tested at −30°C and 25.4 cm/s (*Fig. 8a*, curves E and F). The solitary CT sample (curve E) experienced a dramatic improvement in ductility with only a slightly lower *K*-value compared with the 10% CT sample (curve A). In the simulated large part, again the sample

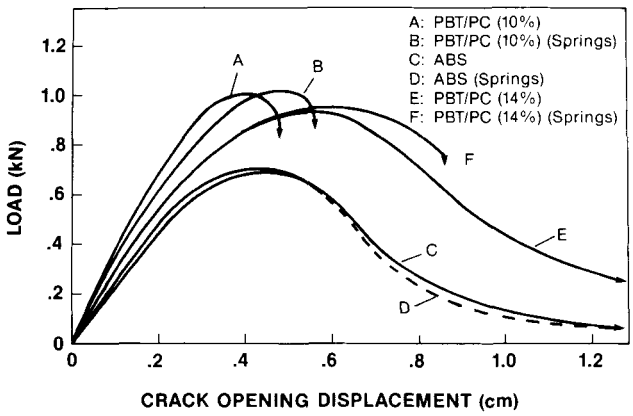

Fig. 8a. Fracture behavior of ABS and PBT/PC (14% rubber) compared with PBT/PC (10% rubber) at 25.4 cm/s and −30°C.

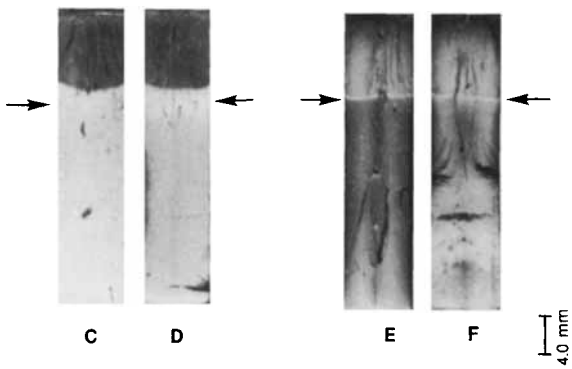

Fig. 8b. Fracture surfaces of ABS and PBT/PC (14% rubber) at −30°C and 25.4 cm/s (see Fig. 5b for fracture surfaces of PBT/PC, 10% rubber.

fractured unstably after initial ductile crack growth, but the unstable fracture was semiductile in appearance in contrast to the brittle unstable behavior observed in the 10% sample at the same conditions. The corresponding fracture surfaces are shown in *Fig. 8b*.

A commercial ABS was also tested at −30°C and 25.4 cm/s to study the behavior of a considerably more compliant polymer (*Fig. 8a*, curves C and D). The simulated large part, although extremely ductile at these same conditions, did exhibit an unstable behavior in that a transition from slow crack growth to fast crack growth occurred just beyond the maximum load as indicated by the dashed line in curve D. The improved large part response, however, was offset by a 32% decrease in peak load compared with the 10% PBT/PC sample.

SUMMARY

1. Large compliant structures were simulated in laboratory tests by placing soft springs in series with compact tension (CT) test samples.
2. At room temperature and slow test rates, rubber-toughened PBT/PC compact tension samples with sharp fatigue cracks fractured in a ductile and stable manner. In the simulated large parts, however, initial ductile crack growth at similar corresponding *K*-values was followed by ductile but unstable failure. This unstable behavior resulted from the inability of the crack to absorb fully the excessive stored strain energy released during initial crack growth.
3. At low temperatures (−30°C) and slow rates, CT samples with fatigue cracks fractured in a ductile and stable fashion. At −30°C and fast rates, brittle unstable failures occurred after ductile crack growth had initiated. In the simulated large parts, however, brittle unstable failures were observed at both rates tested, with the unstable failures again preceded by initial ductile crack growth. Even though brittle fracture was observed, the onset of crack initiation occurred at *K*-values similar to those of ductile, stable fracture.
4. Samples with blunt crack tips behaved similarly to those with sharp fatigue cracks.
5. Increasing the rubber content in the PBT/PC blend prevented any brittle failures at low temperatures and fast rates. The simulated large part fractured in a semiductile unstable manner. The dramatic improvement in ductility resulted in only a slightly lower *K*-value.
6. A considerably more compliant polymer, ABS, was similarly tested at low temperatures and fast rates. The simulated large part, although extremely ductile at these conditions, did exhibit an unstable behavior. The improved large part response was offset by a drastic reduction in *K*-value, however.

7. This unstable, possibly catastrophic behavior exhibited by the simulated large parts is exemplary of the behavior that has been observed in actual large parts. The physical conditions at which these instabilities occur varies with the relative size and thickness of the part and the inherent toughness of the material.

CONCLUDING REMARKS

These results demonstrate that the fracture behavior of small test samples does not always reflect the actual fracture behavior of large parts. Small test samples *do* reflect large part response when brittle, unstable fracture takes place. Under these conditions, the propagating crack tip is only influenced by the local stress field, and not by global effects. Therefore, brittle fractures are expected in large parts loaded to the same local crack tip conditions. However, small test samples *do not* necessarily reflect large part response when ductile stable crack growth occurs. Under these conditions, global effects can become important. When the local crack tip propagates, globally stored strain energy can be released, the amount of which depends on the total system compliance. This released energy is the driving force for crack growth; thus larger, more compliant parts that can store (and release) large amounts of strain energy can produce highly unstable fractures. Although the crack propagation may have been

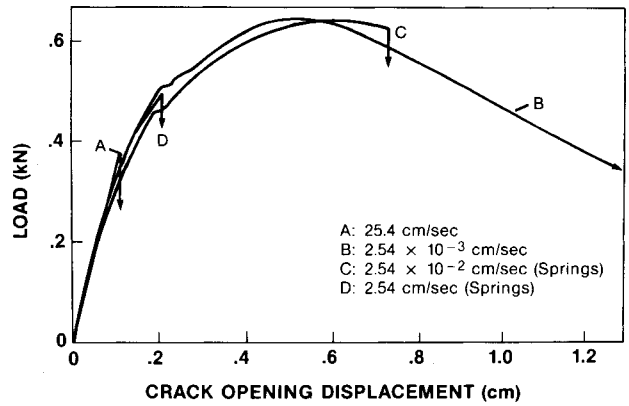

Fig. A-1. Fracture behavior of polycarbonate at 25°C: (A) brittle, (B) ductile, (C) ductile unstable, and (D) brittle unstable.

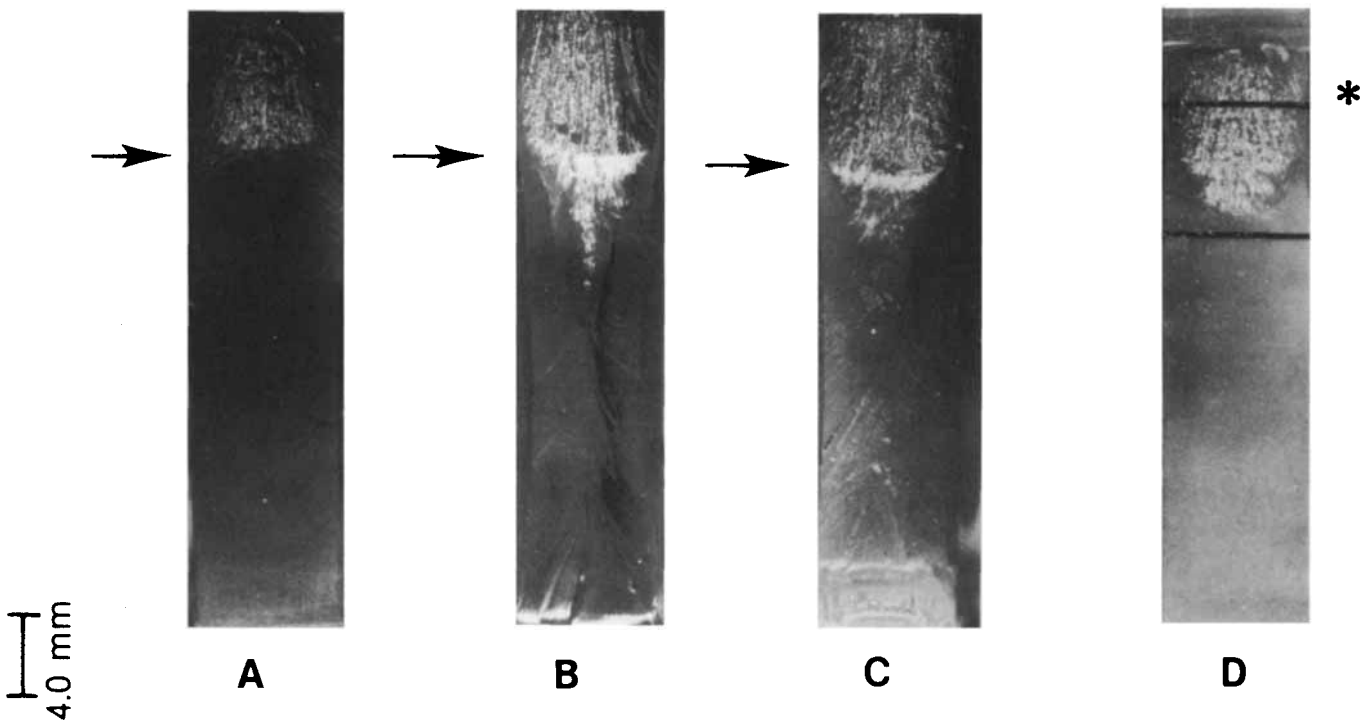

→ Designates end of fatigue

A: BRITTLE
B: DUCTILE
C: DUCTILE UNSTABLE WITH SPRINGS
D: BRITTLE UNSTABLE WITH SPRINGS

* See Figure A-3 for enlargement of this area

Fig. A-2. Polycarbonate fracture surfaces at 25°C.

initially ductile, the subsequent instability could lead to unstable brittle fracture.

These conclusions have major implications for the interpretation of the fracture behavior of large structural plastic parts. When unstable brittle fractures are observed under conditions that normally lead to ductile failures, it may be erroneous to classify immediately the failure as a truly brittle failure. The initial crack growth region should be carefully examined to see if ductile crack growth had preceded the brittle instability. If this were the case, the initial ductile strength and toughness values could have been retained. This information is critical to the proper design of large structural parts.

APPENDIX A

Polycarbonate Fracture Behavior

Polycarbonate was tested to clarify the distinction between brittle fracture, ductile fracture, and the unstable behavior that can result from high energy storage. Testing was conducted in accordance with the test technique described in *Experimental* in the body of the report. Representative results at room temperature (25°C) are presented in *Fig. A-1*. The fracture surfaces are shown in *Figs. A-2* and *A-3*. A completely brittle fracture of the solitary CT sample was achieved at the piston displacement rate of 25.4 cm/s (*Fig. A-1*, curve A). Under these conditions, the load varied linearly with the crack opening displacement until rapid fracture at a K-value of 2.9 MN/m$^{3/2}$ (true brittle failure).

A completely ductile fracture of the solitary polycarbonate CT sample was achieved at 2.54×10^{-3} cm/s (*Fig. A-1*, curve B). A K-value of 4.9 MN/m$^{3/2}$ was reached at the peak load with a subsequent gradual decrease from maximum to zero load (ductile stable failure). Fracture of the CT sample in series with springs at a piston displacement rate of 2.54×10^{-2} cm/s resulted in a similar K-value of 5.0 MN/m$^{3/2}$ (*Fig. A-1*, curve C). However, almost immediately after the maximum load was reached, the sample experienced a rapid drop to zero load, while retaining the full ductile fracture surface appearance similar to that of the sample represented by curve B. This behavior is referred to as ductile unstable failure. Although the sample fractured unstably, the fracture behavior before instability was nearly identical to the stable, ductile failure of curve B.

A more drastic unstable behavior was achieved by fracture of the CT sample in series with the springs at a rate of 2.54 cm/s (*Fig. A-1*, curve D). The sample initially experienced a limited amount of ductile stable growth and then a rapid brittle fracture at an intermediate K-value of 3.8 MN/m$^{3/2}$. This rapid brittle frac-

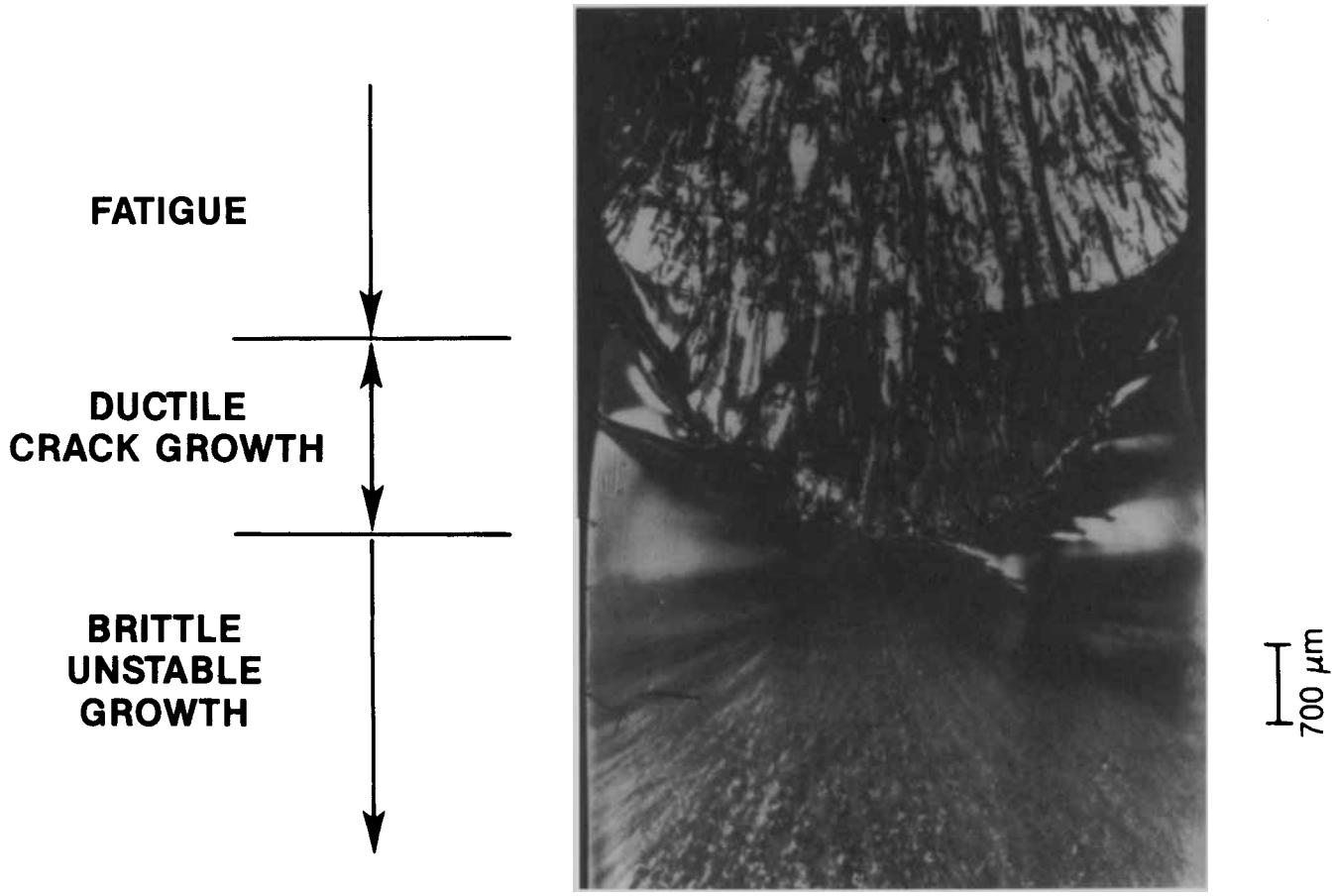

Fig. A-3. Enlarged portion of polycarbonate sample D.

ture is referred to as brittle unstable failure in contrast to ductile unstable failure (refer to the fracture surfaces of *Figs. A-2* and *A-3*). Again, the sample compliance behavior before the point of instability is identical to curves B and C. These results are direct evidence that the unstable failure in the presence of the springs does not occur because of inherent brittleness but is, in fact, a direct result of the high energy storage in the springs.

APPENDIX B

Instability

A simple graphical construction can be used to illustrate the instability condition described in the main text. In this conceptualization, we separate the local area around the crack tip from the global regions far from the crack tip. The local and global regions are considered to support the same load (a series model). *Figure B-1* shows a graphical representation of the loaded sample for the linear elastic case. The areas of the two triangles represent the stored elastic energy within the local and the global regions. For the example shown in *Fig. B-1*, the global region stores considerably more energy (a large sample).

In *Fig. B-2*, a ductile response is shown for the local region (or equivalently, for a small sample or a sample in an infinitely stiff system). In *Fig. B-3*, the load displacement response for the global region is introduced. If we suppose that we are at position A, with a crack of length a, the local region has compliance given by the inverse of the slope of the straight line OA. The total stored strain energy is given by the area of the triangle OAP (where P is at the origin for the plot of the global region). For a fixed displacement condition, if we allow the crack to grow a distance, da, the local region compliance

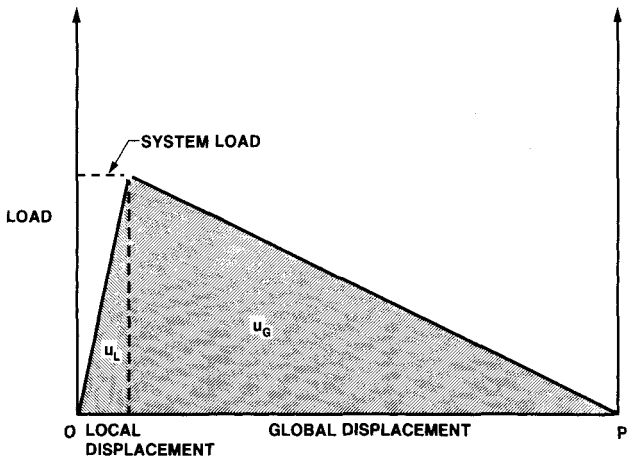

Fig. B-1. Stored elastic energy for the local and the global regions (or for a sample and spring in series) in the linear elastic regime; u_L = stored strain energy in the local region. u_G = stored strain energy in the global region. The total displacement is equal to the sum of the local and the global displacements. Note the different origins (O and P) for the local and global regions.

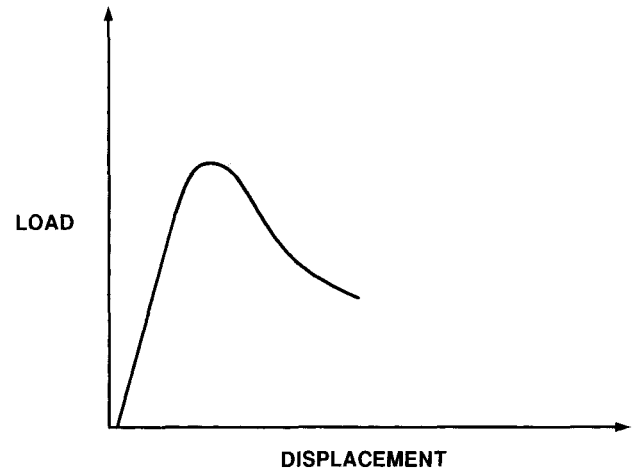

Fig. B-2. Ductile response for the local region (or of a small sample).

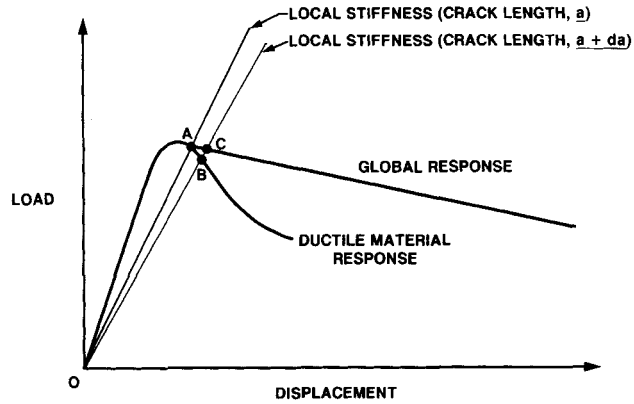

Fig. B-3. Crack instability. To have crack growth da, at fixed total displacement, AC is the actual (necessary) path, but AB is the sufficient path for ductile crack growth. The excess strain energy released is given by the triangle ACB, and this can lead to the crack instability.

is represented by line OB. However, because of the presence of the global regions, the load trace will not follow the path AB, but instead is forced to traverse AC. The strain energy release necessary for crack propagation by da is given by the area within OABO, but the actual energy released by the entire system is given by OACBO, which exceeds the necessary amount by area ACB. Thus, excess energy is released and the crack will grow. As the sample compliance increases, the area ACB will likewise increase. This leads to the fracture instability. The limiting point for instability is associated with the point where the ductile load curve is tangent to the global line; i.e., when the area ACB vanishes.

ACKNOWLEDGMENTS

John Maxam of General Electric is gratefully acknowledged for his manufacture of the injection-molded plaques. Estelle Sauter of General Electric is also gratefully acknowledged for her photography work. One of the authors (Michael

Takemori) benefited considerably from discussions with Drs. Tetsuo Shoji and Masumi Saka of Tohoku University, Sendai, Japan.

REFERENCES

1. ASTM Test Standard E399-83, "Standard Test Method for Plane-Strain Fracture Toughness of Metallic Materials," Annual Book of ASTM Standards, Section 2, p. 779 ASTM, Philadelphia (1983).
2. J. McGuire and M. T. Takemori, "Fracture Instability in Large Structural Plastic Parts," General Electric Memo Report No. MOR-85-114 (1985).
3. M. T. Takemori and J. M. McGuire, *Am. Chem. Soc., Div. Polym. Chem. Polym. Prepr.* **26**, 149 (1985).